ACS SyntheticBiology
Letter
Cite This: ACS Synth. Biol. 2018, 7, 371−376
pubs.acs.org/synthbio

Analyzing and Tuning Ribozyme Activity by Deep Sequencing To Modulate Gene Expression Level in Mammalian Cells

Shungo Kobori and Yohei Yokobayashi*

Nucleic Acid Chemistry and Engineering Unit, Okinawa Institute of Science and Technology Graduate University, Onna, Okinawa 904 0495, Japan

Supporting Information

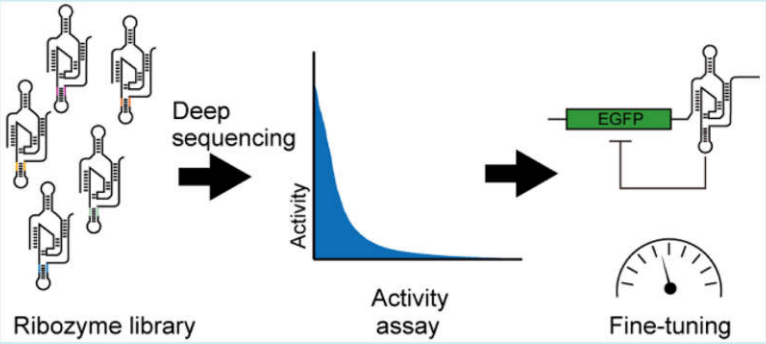

ABSTRACT: Self-cleaving ribozymes, in combination with aptamers and various classes of RNAs, have been heavily engineered to create RNA devices to control gene expression. Although understanding of sequence−function relationships of ribozymes is critical for such efforts, our current knowledge of self-cleaving ribozymes is mostly limited to the results from small scale mutational studies performed under different conditions, or qualitative results of mutate-and-select experiments that may contain experimental biases. Here, we applied our strategy based on deep sequencing to comprehensively assay a large number of mutants to systematically examine the effect of the P4 stem sequence on the activity of an HDV-like ribozyme. We discovered that the ribozyme activity is highly sensitive to the sequence and the apparent stability of the varied positions. Furthermore, we demonstrated that the collection of the ribozyme variants with different activities can be used as a convenient device to fine-tune the level of gene expression in mammalian cells.

KEYWORDS: *RNA engineering, ribozyme, deep sequencing*

Self-cleaving ribozymes have proved to be versatile tools in synthetic biology. Most notably, engineered allosteric aptazymes comprised of a self-cleaving ribozyme and an RNA aptamer have been exploited to achieve chemical regulation of gene expression *via* a variety of mechanisms in prokaryotic and eukaryotic cells.[1,2] Following the seminal work from the Mulligan group that demonstrated gene repression and regulation by a hammerhead ribozyme inserted in the noncoding regions of mammalian mRNAs,[3] a variety of synthetic gene switches based on self-cleaving aptazymes were developed in bacteria,[4,5] yeast,[6] and mammalian cells.[7] Although a limited number of self-cleaving ribozymes have been known and studied for decades, recent computational efforts led to the discovery of new instances and new classes of ribozymes in all kingdoms of life,[8−10] fueling the excitement for broader applications of ribozymes in synthetic biology. However, applications of ribozymes reported to date have only tapped a tiny fraction of the potentially useful natural and artificial sequences. Furthermore, basic understanding of how the ribozyme sequence and structure affect its catalytic activity is also critical for engineering efficient RNA devices.

This work focuses on a hepatitis delta virus (HDV)-like ribozyme drz-Agam-2−1 from the mosquito *Anopheles gambiae* (Figure 1a). This ribozyme is one of the new HDV-like ribozymes identified by computational search of genome sequence data[8] which we later used to engineer aptazymes to control gene expression in mammalian cells.[11] Earlier studies on the original HDV ribozymes have shown that the P4 stem is not essential but does influence the catalytic activity.[12,13] In these studies, the P4 stem of the HDV ribozyme was replaced with two or three bridging nucleotides which resulted in functional, albeit 10- to 100-fold less active, ribozymes. More recently, Webb and Lupták identified a natural ribozyme drz-Hdis-1 from the Pacific abalone (*Haliotis discus*) that only contains a 5-nt linker in the P4 stem region which is unlikely to form a stable structure.[14] We and others have replaced P4 with an aptamer to engineer allosteric HDV ribozymes.[11,15,16] These results suggest that the sequence and stability of the P4 stem strongly affect the ribozyme activity, but the sequence-function

Received: October 13, 2017
Published: January 17, 2018

DOI: 10.1021/acssynbio.7b00367
ACS Synth. Biol. 2018, 7, 371−376

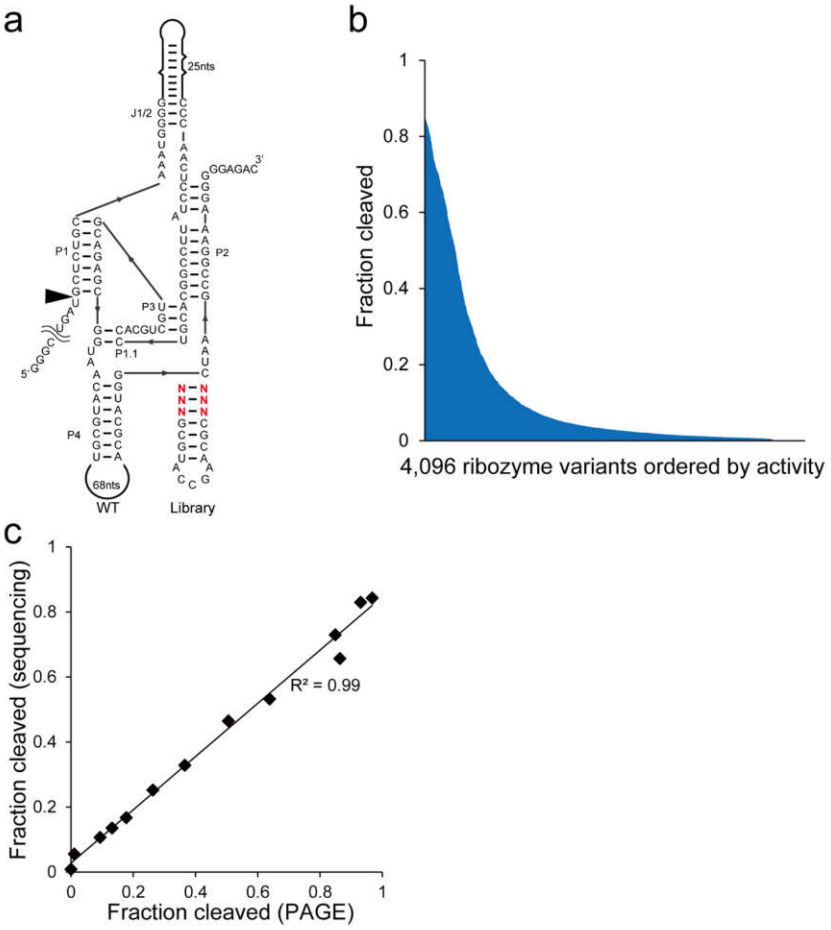

Figure 1. Structure and activity of ribozyme mutants. (a) Ribozyme library based on the HDV-like ribozyme in *A. gambiae* drz-Agam-2−1.[8] Randomized bases are shown in red. (b) Activities of 4096 ribozyme variants in the library measured by deep sequencing ordered by FC. (c) Correlation of FC values derived from deep sequencing and PAGE of 13 selected ribozyme variants from the library. Two measurements by PAGE were performed for each variant.

relationship of P4 in HDV-like ribozymes has not been studied systematically.

Conventional mutagenic studies of ribozymes require design, synthesis, and characterization of individual ribozyme mutants, limiting the number of ribozyme variants that could be studied under the same condition. We recently reported a high-throughput ribozyme assay strategy based on deep sequencing which allows simultaneous assay of $>10^4$ ribozyme variants.[17,18] In this work, we applied the strategy to comprehensively assay all 4096 ($= 4^6$) variants of drz-Agam-2−1 in which the three base pairs in P4 proximal to the ribozyme core were varied (Figure 1a). The results provide a semiquantitative understanding of the influence of the local P4 structure on the ribozyme activity.

Our massively parallel assay also yielded a rich collection of ribozyme sequences with diverse catalytic activities. We sought to exploit these ribozyme mutants as RNA devices for fine-tuning gene expression. Optimization of gene expression level is critical for many synthetic biology applications. Unnecessary overexpression can result in metabolic burden and pleiotropic effects. Several straightforward strategies exist for fine-tuning of gene expression level in bacteria, such as varying promoter and ribosome binding site (RBS) sequences. For example, the Anderson promoter collection[19] serves as a useful toolbox of constitutive *Escherichia coli* promoters with a wide range of strengths. Analogous user-friendly tools for modulating mammalian gene expression should benefit those interested in synthetic biology of mammalian cells. However, mammalian promoters are significantly more complex compared to prokaryotic promoters, limiting the generality and practical utility of synthetic promoters.[20] Consequently, we explored the possibility of using the collection of drz-Agam-2−1 mutants as a small RNA device to modulate mammalian gene expression by inserting the ribozyme in the 3′ UTR of a reporter gene mRNA. We envision that well characterized ribozyme variants such as those described in this study will be useful for fine-tuning gene expression levels in mammalian cells.

RESULTS AND DISCUSSION

We designed a ribozyme library based on an HDV-like ribozyme drz-Agam-2−1 found in *A. gambiae*.[8] The wild-type ribozyme contains a 7-bp P4 stem with a rather long (68 nt) sequence in the loop region which was truncated to a short 5-nt loop (Figure 1a). Previous reports on HDV ribozymes showed that although the P4 structure is not functionally essential, its sequence affects the ribozyme activity.[11,12] One likely scenario is that the P4 affects the local stability of the neighboring catalytic core which then modulates catalytic efficiency.

DOI: 10.1021/acssynbio.7b00367
ACS Synth. Biol. 2018, 7, 371−376

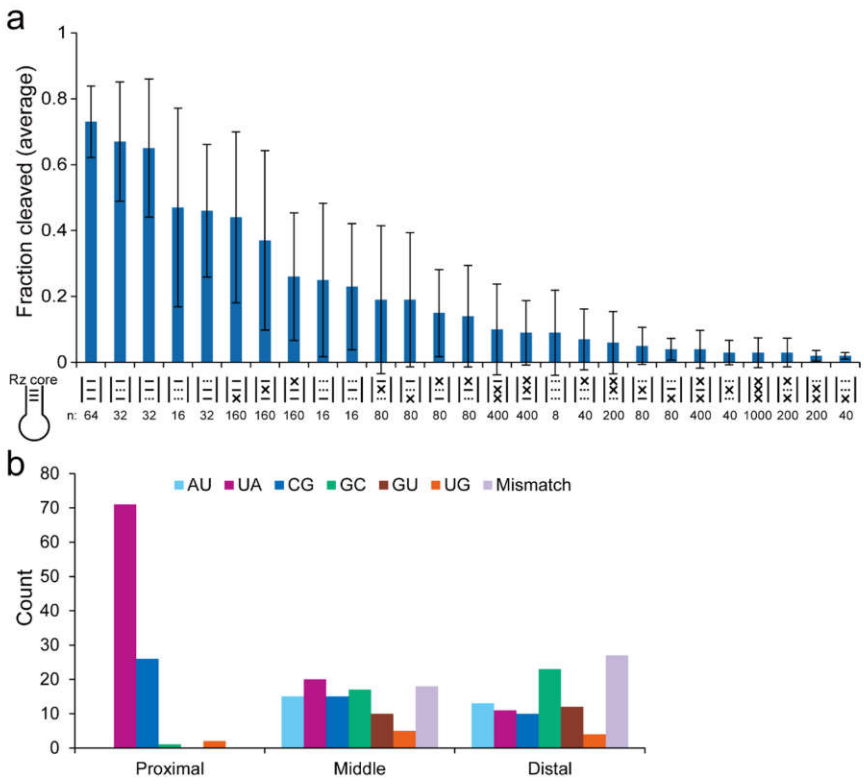

Figure 2. Sequence-function relationship of the P4 stem. (a) Average activities (FC) of the library subpopulations categorized by the apparent base pairing pattern. "*x*" indicates a mismatch, "–" indicates Watson–Crick base pair (A-U/U-A or G-C/C-G), and "···" indicates a wobble base pair (G-U/U-G). *n*: number of variants in each subpopulation. The data shown are mean ± standard deviation (SD). (b) Frequencies of specific base pairs (or lack thereof) at the randomized positions (proximal, middle, and distal, relative to the ribozyme core) of highly active mutants with FC > 0.75.

Therefore, varying the identity of the P4 nucleotides that are proximal to the ribozyme core was envisioned to influence the ribozyme activity. To this end, a ribozyme library in which 6 nt shown in Figure 1a were randomized was constructed by PCR using degenerate oligonucleotides.

The library was constructed as a dsDNA template for *in vitro* transcription by T7 RNA polymerase. The library template was transcribed *in vitro* with low Mg^{2+} concentration (3 mM) for 3 h at 37 °C during which some ribozymes self-cleaved cotranscriptionally. The use of a low Mg^{2+} concentration during *in vitro* transcription was found to more accurately reflect the ribozyme activity in mammalian cells in our previous work,[11] possibly because it more closely represents the intracellularly available Mg^{2+}. It has also been shown that cotranscriptional activity of the HDV ribozyme, rather than the activity of the full length ribozyme, better explains the biological activity of HDV ribozyme mutants.[21]

The ribozymes were reverse-transcribed into cDNAs along with a template-switching oligonucleotide (TSO) to attach partial adapter sequences required for deep sequencing. Finally, PCR was performed to add the complete adapter sequences to prepare the sequencing sample. Deep sequencing of the library yielded approximately 13.5 million reads. On average, each one of the 4096 mutants had 3295 reads. Each read can be determined cleaved or uncleaved based on the sequence at the predicted cleavage site which were counted for all mutants. For each ribozyme mutant, its activity can be expressed as fraction cleaved (FC), which is calculated as follows:

$$FC = n_c/(n_c + n_{unc})$$

where n_c and n_{unc} are the read counts of the cleaved and uncleaved fragments, respectively. To visualize the range of activities of the ribozyme variants, FC values of all 4096 mutants were ordered by FC and plotted as shown in Figure 1b. We observed a broad range of activities with FC ranging from 0.028 to 0.864. This is consistent with the assumption that P4 structure affects ribozyme activity but is not functionally essential.

Next, to validate the FC values measured by deep sequencing, we selected 13 ribozyme variants with a range of activities (based on deep sequencing) and individually measured their activities by conventional polyacrylamide gel electrophoresis (PAGE). The FC values obtained by the two methods showed an excellent correlation (R^2 = 0.99) (Figure 1c) in agreement with our previous reports.[11,17,18]

To test the hypothesis that the stability of the P4 stem proximal to the ribozyme core is beneficial for activity, we analyzed subpopulations of the variants categorized according to the presence or absence of base-pairing at the randomized positions. As expected, the 64 variants that can be expected to form canonical Watson–Crick base pairs at all three positions showed, on average, the highest FC values. The next four most active subpopulations contain a mix of Watson–Crick and wobble base pairs, further underscoring the importance of the P4 stem structure. A potentially interesting trend can be observed for the subpopulations with two Watson–Crick pairs and one mismatch. The average FC values decreases as the position of the mismatch moves closer to the ribozyme core (Figure 2a). This may indicate that the destabilizing effect of mismatch, on average, becomes more pronounced when it is

DOI: 10.1021/acssynbio.7b00367
ACS Synth. Biol. 2018, 7, 371–376

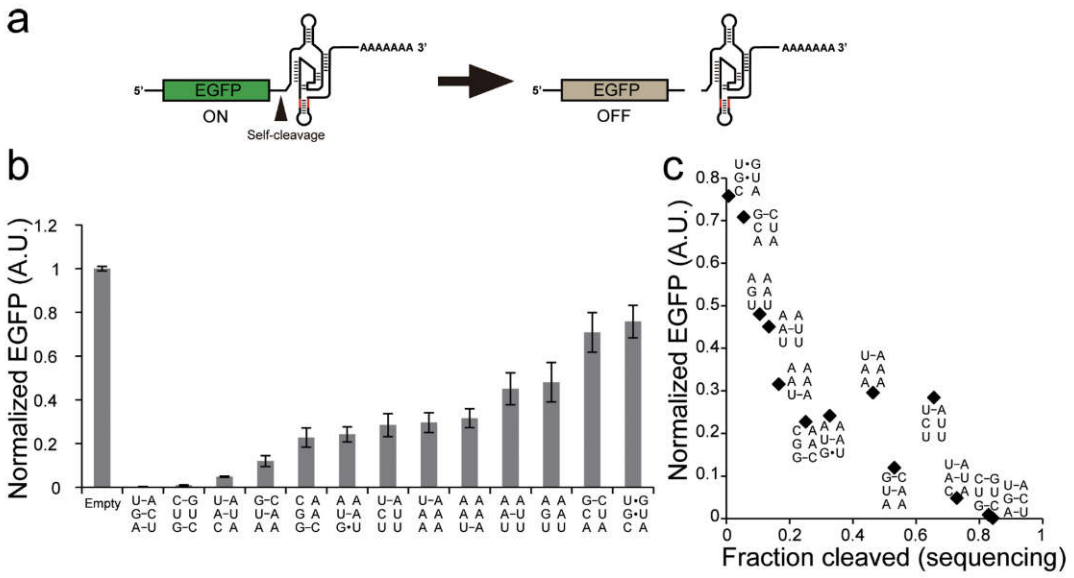

Figure 3. Modulation of gene expression in mammalian cells by self-cleaving ribozyme variants. (a) Schematic illustration of the mechanism of gene expression regulation using ribozyme variants. A ribozyme variant is embedded in the 3′ UTR of a reporter gene (EGFP) mRNA. Ribozyme cleavage results in low EGFP expression due to the detachment of the poly(A) sequence from the coding region. (b) Expression of EGFP in the HEK293 cells transfected with EGFP-ribozyme expression plasmids. EGFP expression is reported relative to the control which lacks the ribozyme (= 1.0, empty), after normalization for transfection efficiency using the cotransfected mCherry expression plasmid. The data shown are mean ± SD from three replicate samples. (c) Correlation of FC values derived from deep sequencing and in vivo EGFP expression of 13 selected ribozyme variants from the library.

closer to the ribozyme core. However, the large variations of the FC values within the subpopulations suggest that a more careful analysis that takes other factors (base identity, stacking energy, *etc.*) into consideration to draw general conclusions. Indeed, an empirical scoring function taking such factors into account has been reported in a recent work from the Farzan group.[22] Upon further analysis of the highly active variants with FC > 0.75, we also found additional preferences for specific base pairs at the position most proximal to the ribozyme core. All but two variants have U-A or C-G at the proximal positions while no such biases were observed in the other positions (Figure 2b).

We previously showed that aptazymes based on the HDV ribozyme assayed under similar conditions by deep sequencing were active when transfected into mammalian cells.[11] Although *in vitro* ribozyme activity does not always translate to intracellular activity, the *in vitro* transcription reaction format resembling the cotranscriptional folding environment as well as the use of a low Mg^{2+} concentration reflecting the physiological condition contribute to the good correlation of the activities *in vitro* and in cells. Therefore, we embedded our drz-Agam-2−1 mutants with a range of *in vitro* activities in the 3′ UTR of the mRNA coding for EGFP (Figure 3a) on a plasmid. Self-cleavage of the ribozyme detaches the poly(A) tail of the mRNA and results in lower protein expression.

Intracellular activities of the ribozyme variants were measured by cotransfecting ribozyme-containing EGFP expression plasmid and mCherry expression plasmid as a control to normalize for variation in transfection efficiency. EGFP expression level was reported relative to that of the parent EGFP plasmid without ribozyme (1.0). As shown in Figure 3b and 3c, there is a good qualitative correlation between *in vitro* ribozyme activity and EGFP expression. Most importantly, the EGFP expression levels span a broad range from 0.002 to 0.76 although the low expression levels of the most active ribozyme mutants should be measured using a more sensitive reporter such as luciferase for more precise quantification. Nevertheless, we propose that a collection of ribozyme mutants such as these may be useful for fine-tuning constitutive expression levels in mammalian cells. A potential advantage of using ribozymes to modulate expression level is their small genetic footprint. Our drz-Agam-2−1 mutants are 125 nt, but even smaller ribozymes can be developed based on other ribozyme classes such as hammerhead and twister ribozymes. Moreover, unlike mammalian promoters which require complex transcriptional machinery that varies among different cell types and states, intrinsic ribozyme activity is expected to be relatively independent of cellular environment. Placement of the ribozyme in the 3′ UTR also allows preservation of native promoters which may be desirable for modulating endogenous gene expression, for example, by genome editing.

Babiskin and Smolke engineered RNase III substrate sequences within the 3′ UTR of mRNA to modulate gene expression in yeast.[23,24] While their strategy also circumvents manipulation of the eukaryotic promoters, gene regulation depends on an additional protein factor (RNase III). Analogous work in mammalian cells has not been reported. Similar strategies that depend on RNA targeting by another protein factor may suffer from potential complications in mammalian cells, for example, differential expression level of the protein factor in various cell types, or interference with the natural function of the protein factor.

In summary, we applied deep sequencing to comprehensively map the local sequence-function landscape of an HDV-like ribozyme. The cotranscriptional self-cleavage results of 4096 variants led to a more general understanding of the sequence and structural requirements of the P4 stem compared to the analysis of a limited number of mutants by conventional

DOI: 10.1021/acssynbio.7b00367
ACS Synth. Biol. 2018, 7, 371−376

Table 1. Oligonucleotides Used in This Study

name	sequence (5′−3′)
Frag-1	TAATACGACTCACTATAGGGCCGCGACTCTAGAAGTGATGCTCTGCAAATGGGGTAGGAGGCGATGCCTCGTCCTCAT ACCCAACTCCTATTCCGGCACGTCCACGTCGTGCAGAGCGGTA
PCR-F1	Biotin-TAATACGACTCACTATAGGGCCGCG
PCR-R1	GTCTCCCCCTTTCCGGC
Lib-N6	GTCTCCCCCTTTCCGGCTTAGCNNNGCGTTCGGTACGCNNNTTACCGCTCTGCACGACGTG
RT-1	CTACACGACGCTCTTCCGATCTTATCCTCTCGACTGTCTCCCCCTTTCCG
RT-2	CTACACGACGCTCTTCCGATCTAGAGTAGACACGACTGTCTCCCCCTTTCCG
TSO[a]	iCiGiC-GAGTTCAGACGTGTGCTCTTCCGATCT-rGrGrG
PCR-F2	AATGATACGGCGACCACCGAGATCTACACACACTCTTTCCCTACACGACGCTCTTCCGATC
PCR-R2	CAAGCAGAAGACGGCATACGAGATCGAGTAATGTGACTGGAGTTCAGACGTGTGCTCTTCC

[a]rG indicates RNA bases. iC and iG are isocytosine and isoguanine, respectively.

assays.[12,13] Furthermore, we exploited the large data set to identify a set of ribozyme variants with diverse activities which can be used to fine-tune mammalian gene expression.

METHODS

Library Preparation. The DNA library used for *in vitro* transcription of ribozyme mutants was constructed using synthetic oligonucleotides and PCR. Oligonucleotide and DNA fragment sequences are listed in Table 1. The oligonucleotide containing degenerate bases (N) was synthesized using the "hand-mix" option (equimolar mixture of all nucleotide phosphoramidites) offered by the manufacturer (GeneDesign, Inc.).

The DNA library was prepared by overlap PCR of the 5′ constant sequence Frag-1 and the 3′ fragment containing the degenerate bases Lib-N6 as templates and PCR-F1 and PCR-R1 as PCR primers. The final PCR products were purified by DNA Clean & Concentrator-5 kit (Zymo Research) and used for *in vitro* transcription. The sequence of the final dsDNA template is as follows (T7 promoter sequence underlined):

5′-TAATACGACTCACTATAGGGCCGCGACTCTAGAAGTGATGCTCTGCAAATGGGGTAGGAGGCGATGCCTCGTCCTCATACCCAACTCCTATTCCGGCACGTCCACGTCGTGCAGAGCGGTAANNNGCGTACCGAACGCNNNGCTAAGCCGGAAAGGGGGAGAC-3′ Because PCR-F1 is biotinylated at its 5′ terminus, the dsDNA template is also biotinylated.

***In Vitro* Transcription.** Ribozymes were transcribed *in vitro* in 200 μL reactions in the transcription buffer (40 mM Tris-HCl pH 8.0, 2 mM spermidine, 10 mM DTT, 3 mM $MgCl_2$) in the presence of a dsDNA template (40 pmol), NTPs (2 mM each), RNase Inhibitor, Murine (320 units, New England Biolabs), and T7 RNA polymerase (500 units, New England Biolabs) for 3 h at 37 °C. The reaction was terminated by adding 20 μL of 100 mM EDTA and incubated with 330 μL of streptavidin-coated magnetic beads (Streptavidin MagneSphere, Promega) for 20 min on ice with consistent pipetting to remove DNA template. The beads were removed and the transcribed RNAs were purified by RNA Clean & Concentrator-5 kit (Zymo Research) and dissolved in 20 μL 10 mM EDTA.

Reverse Transcription and Template Switching Reactions. The transcribed and purified RNA mixture (2.5 pmol) was mixed with 50 pmol of RT-1 and RT-2 (Table 1) and dNTPs (3.36 mM each) in 4.5 μL and heated to 72 °C for 3 min and placed on ice. Reverse transcription was initiated by adding 19.2 μL of RT solution: 84 mM Tris, pH 8.3, 126 mM KCl, 14.82 mM $MgCl_2$, 8.4 mM DTT, 20 unit of RNase Inhibitor, Murine (New England Biolabs), 13% PEG, 12.6 units/μL of Maxima H Minus Reverse Transcriptase (Thermo Fisher Scientific), and 13 μM TSO (Table 1). The solution was kept at 42 °C for 1 h, then at 60 °C for 2 min, and finally at 37 °C for 2 h. The reaction was stopped by adding 2.5 μL NaOH solution (2.5 M) and heating (95 °C for 3 min). The cDNAs were first cleaned by Oligo Clean & Concentrator kit (Zymo Research), purified by denaturing PAGE (6% polyacrylamide, 8 M urea, 19:1 acrylamide: bis(acrylamide)), and eluted by electroelution. The purified cDNAs were dissolved in 10 μL water. The sequencing library was generated by PCR with primers PCR-F2 and PCR-R2 (Table 1) using NEBNext Ultra II Q5Master Mix (New England Biolabs) in a 50 μL reaction containing 2.5 μL cDNAs and 0.5 μM each primer. The PCR reaction was performed in seven cycles of 3 min at 98 °C followed by 80 s at 65 °C. The PCR products were purified by agarose gel electrophoresis using Zymoclean Gel DNA Recovery Kit (Zymo Research).

Sequencing and Data Analysis. Sequencing was performed by OIST DNA Sequencing Section. The library was analyzed on Illumina HiSeq 2500 (180 cycles, single-end) along with other indexed samples and PhiX. The sequencing data were analyzed with custom Perl scripts unless otherwise noted. First, the raw reads were filtered by NGS QC Toolkit v2.3.3 to remove low quality reads that contain more than 30% base calls with Phred score (Q-score) below 20. The reads were sorted based on the index and the barcode sequences to determine whether the original transcript was cleaved or uncleaved, and sorted according to the sequence in the randomized region.

Ribozyme Assay by PAGE. Individual ribozyme mutants tested were first cloned in a plasmid and sequence verified. The plasmids were used to prepare *in vitro* transcription templates by PCR using Phusion High-Fidelity 2X Master Mix (New England Biolabs). *In vitro* transcription reactions were performed under the same conditions as the library construction in 10 μL scale. The transcribed RNAs were separated by 8% denaturing PAGE and stained by SYBR Gold (Thermo Fisher Scientific). The gels were photographed and analyzed using SE-6100 LuminoGraph I (ATTO).

Ribozyme Assay in Mammalian Cells. Ribozyme sequences were cloned in the 3′ UTR of the EGFP transcript in pEGFP-N1-BspEI as previously described.[15] HEK293 cells were maintained in a 5% CO_2 humidified incubator at 37 °C in Dulbecco's modified Eagle's medium (DMEM) (Wako) supplemented with 10% fetal bovine serum (FBS) (Gibco) and 1× antibiotic-antimycotic (Wako). One day before transfection, HEK293 cells were trypsinized and diluted

DOI: 10.1021/acssynbio.7b00367
ACS Synth. Biol. 2018, 7, 371−376

appropriately with fresh complete medium, and 2.4×10^4 cells/well (~100 μL) were seeded onto 96-well plates. EGFP-ribozyme plasmid (340 ng) and pCMV-mCherry (170 ng) which constitutively expresses mCherry were cotransfected with 3.4 μL of PolyFect reagent (QIAGEN) per well according to the manufacturer's instruction. After 4 h incubation, the medium was replaced with 100 μL fresh complete medium. The cells were incubated for additional 21 h before EGFP assay.

Cellular fluorescence was measured and normalized according to our previous report.[15] Briefly, the cell culture medium was replaced with phosphate buffered saline (PBS) (150 μL per well) and incubated at 37 °C until measurement. Fluorescence intensities were measured for EGFP (484 nm excitation/510 nm emission/10 nm bandwidth) and mCherry (587 nm excitation/610 nm emission/10 nm bandwidth) using M1000PRO microplate reader (Tecan). The raw fluorescence values were first subtracted with that of the untransfected cells (background). For each well, EGFP fluorescence was normalized by mCherry ([EGFP fluorescence]/[mCherry fluorescence]) to account for variations in transfection efficiency. The values were further normalized by the cells transfected with pEGFP-N1-BspEI (= 1.0). The reported values are mean ± SD from three replicate samples.

■ ASSOCIATED CONTENT

Supporting Information

The Supporting Information is available free of charge on the ACS Publications website at DOI: 10.1021/acssynbio.7b00367.

Ribozyme activities of all variants acquired by deep sequencing (XLSX)

■ AUTHOR INFORMATION

Corresponding Author

*E-mail: yohei.yokobayashi@oist.jp.

ORCID

Shungo Kobori: 0000-0003-4995-5847

Yohei Yokobayashi: 0000-0002-2417-1934

Notes

The authors declare no competing financial interest.

■ ACKNOWLEDGMENTS

We thank Dr. Hiroki Goto and OIST DNA Sequencing Section for sequencing support. The research was funded by Okinawa Institute of Science and Technology Graduate University.

■ REFERENCES

(1) Groher, F., and Suess, B. (2014) Synthetic riboswitches - A tool comes of age. *Biochim. Biophys. Acta, Gene Regul. Mech. 1839*, 964–973.

(2) Felletti, M., and Hartig, J. S. (2017) Ligand-dependent ribozymes. *Wiley Interdiscip. Rev.: RNA 8*, e1395.

(3) Yen, L., Svendsen, J., Lee, J.-S., Gray, J. T., Magnier, M., Baba, T., D'Amato, R. J., and Mulligan, R. C. (2004) Exogenous control of mammalian gene expression through modulation of RNA self-cleavage. *Nature 431*, 471–476.

(4) Ogawa, A., and Maeda, M. (2008) An Artificial Aptazyme-Based Riboswitch and its Cascading System in E. coli. *ChemBioChem 9*, 206–209.

(5) Wieland, M., and Hartig, J. S. (2008) Improved aptazyme design and in vivo screening enable riboswitching in bacteria. *Angew. Chem., Int. Ed. 47*, 2604–2607.

(6) Win, M. N., and Smolke, C. D. (2007) A modular and extensible RNA-based gene-regulatory platform for engineering cellular function. *Proc. Natl. Acad. Sci. U. S. A. 104*, 14283–14288.

(7) Kumar, D., An, C.-I., and Yokobayashi, Y. (2009) Conditional RNA Interference Mediated by Allosteric Ribozyme. *J. Am. Chem. Soc. 131*, 13906–13907.

(8) Webb, C.-H. T., Riccitelli, N. J., Ruminski, D. J., and Lupták, A. (2009) Widespread Occurrence of Self-Cleaving Ribozymes. *Science 326*, 953.

(9) Roth, A., Weinberg, Z., Chen, A. G., Kim, P. B., Ames, T. D., and Breaker, R. R. (2014) A widespread self-cleaving ribozyme class is revealed by bioinformatics. *Nat. Chem. Biol. 10*, 56–60.

(10) Weinberg, Z., Kim, P. B., Chen, T. H., Li, S., Harris, K. A., Lünse, C. E., and Breaker, R. R. (2015) New classes of self-cleaving ribozymes revealed by comparative genomics analysis. *Nat. Chem. Biol. 11*, 606–610.

(11) Kobori, S., Nomura, Y., Miu, A., and Yokobayashi, Y. (2015) High-throughput assay and engineering of self-cleaving ribozymes by sequencing. *Nucleic Acids Res. 43*, e85.

(12) Been, M. D., Perrotta, A. T., and Rosenstein, S. P. (1992) Secondary structure of the self-cleaving RNA of hepatitis delta virus: applications to catalytic RNA design. *Biochemistry 31*, 11843–11852.

(13) Thill, G., Vasseur, M., and Tanner, N. K. (1993) Structural and sequence elements required for the self-cleaving activity of the hepatitis delta virus ribozyme. *Biochemistry 32*, 4254–4262.

(14) Webb, C.-H. T., and Luptak, A. (2011) HDV-like self-cleaving ribozymes. *RNA Biol. 8*, 719–727.

(15) Nomura, Y., Zhou, L., Miu, A., and Yokobayashi, Y. (2013) Controlling mammalian gene expression by allosteric hepatitis delta virus ribozymes. *ACS Synth. Biol. 2*, 684–689.

(16) Kertsburg, A., and Soukup, G. A. (2002) A versatile communication module for controlling RNA folding and catalysis. *Nucleic Acids Res. 30*, 4599–4606.

(17) Kobori, S., and Yokobayashi, Y. (2016) High-throughput mutational analysis of a twister ribozyme. *Angew. Chem., Int. Ed. 55*, 10354–10357.

(18) Kobori, S., Takahashi, K., and Yokobayashi, Y. (2017) Deep sequencing analysis of aptazyme variants based on a pistol ribozyme. *ACS Synth. Biol. 6*, 1283–1288.

(19) Anderson promoter collection: http://parts.igem.org/Promoters/Catalog/Anderson, accessed January 17, 2018.

(20) Tornøe, J., Kusk, P., Johansen, T. E., and Jensen, P. R. (2002) Generation of a synthetic mammalian promoter library by modification of sequences spacing transcription factor binding sites. *Gene 297*, 21–32.

(21) Chadalavada, D. M., Cerrone-Szakal, A. L., and Bevilacqua, P. C. (2007) Wild-type is the optimal sequence of the HDV ribozyme under cotranscriptional conditions. *RNA 13*, 2189–2201.

(22) Zhong, G., Wang, H., Bailey, C. C., Gao, G., and Farzan, M. (2016) Rational design of aptazyme riboswitches for efficient control of gene expression in mammalian cells. *eLife 5*, e18858.

(23) Babiskin, A. H., and Smolke, C. D. (2011) A synthetic library of RNA control modules for predictable tuning of gene expression in yeast. *Mol. Syst. Biol. 7*, 471.

(24) Babiskin, A. H., and Smolke, C. D. (2011) Engineering ligand-responsive RNA controllers in yeast through the assembly of RNase III tuning modules. *Nucleic Acids Res. 39*, 5299–5311.